η²-Coordination in pentacoordinate iron complexes

Reiner Birk, Heinz Berke *, Hans-Ulrich Hund,

Anorganisch-chemisches Institut der Universität Zürich, Winterthurerstrasse 190, 8057 Zürich (Switzerland)

Gottfried Huttner, Laszlo Zsolnai,

Anorganisch-Chemisches Institut der Universität Heidelberg, Im Neuenheimer Feld 270, 6900 Heidelberg (F.R.G.)

Lutz Dahlenburg, Ulrich Behrens and Thomas Sielisch

Institut für Anorganische und Angewandte Chemie der Universität Hamburg, Martin-Luther-King-Platz 6, 2000 Hamburg 13 (F.R.G.)

(Received March 3rd, 1989)

Abstract

The reactions of the dinitrogen complexes μ-$N_2[Fe(CO)_2L_2]_2$ (L = $P(OMe)_3$, **1a**; $P(O$-i-Pr$)_3$, **1b**; PEt_3, **1c**) with diphenylketene diphenyl-*p*-tolylketene imine and propionitrile give the η^2-C,O ketene compounds $Fe(CO)_2L_2Ph_2C_2O$ (L = $P(OMe)_3$, **2a**; $P(O$-i-Pr$)_3$, **2b**; PEt_3, **2c**) a ketene imine system $Fe(CO)_2[P(OMe)_3]_2Ph_2C_2N$-*p*-tolyl (**3**) and the propionitrile substitution derivatives $Fe(CO)_2L_2EtCN$ (L = $P(OMe)_3$, **4**; PEt_3, **5**), respectively. The structures of **2c**, **3** and **5a** have been determined by X-ray diffraction.

Introduction

In previous papers we have reported on the bonding abilities of $Fe(CO)_2L_2$ fragments (L = phosphite donor) towards small molecules [1,2]. Our intention in continuing this work was to explore the coordination mode of substituted ketenes, ketene imine and nitriles. In principle, these molecules could show ambivalent ligand behaviour (either η^2-C,C or η^2-C,O bonding modes [3,4a–d] and η^1-N or η^2-N,C [4e] coordination, respectively). All these systems would, therefore, act as probes for the binding preferences of such iron centres.

---

* To whom correspondence should be addressed.

Results and discussion

The simplest routes to ketene, ketene imine or nitrile complexes should follow reaction paths which involve replacement of labile ligands. In the area of carbonyl phosphite iron chemistry we have utilized μ-dinitrogen complexes to generate $Fe(CO)_2L_2$ fragments [5]. As indicated in eq. 1, μ-$N_2[Fe(CO)_2L_2]_2$ (L = $P(OMe)_3$, **1a**; L = PEt_3, **1c**) were obtained by photolysis of the corresponding $Fe(CO)_3L_2$ precursor under N_2, and the isopropylphosphite derivative **1b** was generated in situ by reduction of $Fe(CO)_2[P(O\text{-i-}Pr)_3]_2I_2$ with activated magnesium [6] in the presence of nitrogen.

$$2Fe(CO)_2[P(O\text{-i-}Pr)_3]_2I_2 \xrightarrow[-MgI_2]{Mg,\,N_2} \quad \underset{L}{\overset{L}{OC\diagdown \underset{|}{\overset{|}{Fe}}\diagup OC}} - N\equiv N - \underset{L}{\overset{L}{\underset{|}{\overset{|}{Fe}}}}\underset{CO}{\overset{CO}{\diagup}} \xleftarrow[-2\,CO]{h\nu,\,N_2} Fe(CO)_3L_2$$

(1)

(1)

$$+2\,Ph_2C\!=\!C\!=\!X \quad -N_2 \qquad\qquad +2\,EtCN \quad -N_2$$

$$\underset{L}{\overset{L}{OC\diagdown\underset{|}{\overset{|}{Fe}}\diagup}}\overset{X}{\underset{C\diagdown}{\overset{|}{|}}}\!\!=\!\!C\!-\!Ph \quad\quad 2\;\underset{L}{\overset{L}{OC\diagdown\underset{|}{\overset{|}{Fe}}\diagup OC}}\!-\!N\equiv C\!-\!Et \;\rightleftharpoons\; 2\;\underset{L}{\overset{L}{OC\diagdown\underset{|}{\overset{|}{Fe}}\diagup OC}}\overset{N}{\underset{C\diagdown Et}{\overset{\|}{|}}}$$

(2, 3)   **(4, 5)**   **(4, 5b)**
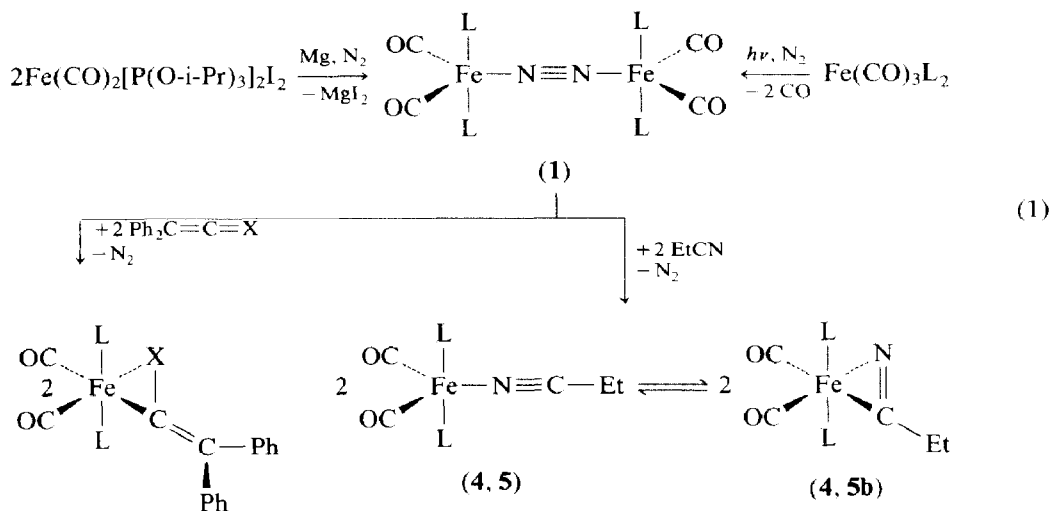
1a, 2a: X = O, L = $P(OMe)_3$ **4**: L = $P(OMe)_3$

1b, 2b: X = O, L = $P(O\text{-i-}Pr)_3$ **5**: L = PEt_3

1c, 2c: X = O, L = PEt_3

    3: X = N-p-tolyl, L = $P(OMe)_3$

When the compounds **1** were allowed to react with diphenylketene (see eq. 1) we were able to isolate crystalline dicarbonylbis(phosphorus-donor)diphenylketene iron complexes (**2a–2c**) in yields of about 90%. Spectroscopic data indicate a trigonal bipyramidal environment around the iron centre, with the ketene ligand in an equatorial position, and it appears that the ketene moieties in compounds **2** remain η^2-C,O-bonded in solution as well as in the solid state. In contrast to these indications for **2c**, IR solution spectroscopic data for **2a** and **2b** suggest the presence in each case of two isomers (two sets of $\nu(C\equiv O)$ bands) (see Table 1). The natural assumption that this isomerism would involve the complexes with η^2-C,O or η^2-C,C ketene ligands would be inconsistent with the presence of only one $\nu(C_2O)$ IR band, located in an absorption region typical of η^2-C,O binding to the metal [4b], and be in disagreement with the ^{13}C NMR observations. Slow or fast interconversions on the NMR time scale in an η^2-C,C $\rightleftharpoons$ η^2-C,O equilibrium, would be expected to give, respectively, three sets or one set of resonances for the phenyl substituents. The presence of two groups of NMR signals for the phenyl protons would most likely be

in accord with pseudo-rotational isomerism at the iron center and a rigidly bonded η^2-C,O ketene moiety which retainins an inside/outside chemical inequivalence of the phenyl residues throughout such a process. EHT calculations on a $(OC)_2[(HO)_3P]_2Fe(H_2C=C=O)$ model indicate small energy differences (≤ 5 kcal/mol) between all possible trigonal bipyramidal isomers. A molecule with one equatorial and one axial phosphorus donor and with the equatorial $P(OH)_3$ group *trans* to the C(ketene) atom has been found to be energetically almost equivalent to the model system with a structure close to that of 2c. This suggests that the rearrangement of 2a,2b would lead, probably via several pseudorotations, to the isomers 2d,2e.
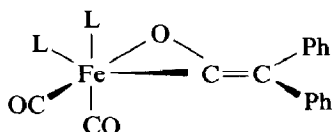
(2d: L = P(OMe)$_3$; 2e: L = P(O-i-Pr)$_3$)

Spectroscopically, there is a strong indication for the involvement of species 2d,2e since IR spectroscopic data are consistent with dicarbonyl units with angles closer to 90° than 180° in both pseudorotomers. In addition there is ^{13}C NMR spectroscopic evidence, as the internal C(ketene) resonances of 2a,2b are split, with higher J(P–C) coupling constants, than the one for 2c (see Table 1). Provided that the isomerisation processes between 2a,2b and 2d,2e are fast on the NMR time scale, the extra coupling contribution in 2a,2b could originate with the interference of the species 2d,2e with a phosphorus ligand in the position *trans* to the C(ketene) atom. Axial/equatorial isomerism in pentacoordinate phosphite substituted iron compounds seems to be a fairly common feature. This has been demonstrated in clear-cut way by the isolation of isomeric iron sulfur dioxide complexes [6b].

The synthesis of 3 was accomplished, as shown in eq. 1, by the facile replacement of the dinitrogen ligand in 1 by two equivalents of diphenyl-*p*-tolylketene imine. The structure of 3 in solution is most probably the same as that determined by X-ray analysis for the solid state. For 3, which is thermally stable, there is no spectroscopic evidence for pseudorotational rearrangements comparable to those inicated for 2a. In solution, as well as in a KBr pellet, the IR spectra show the same ν(C≡O) features, which are consistent with a *cis*-carbonyl arrangement. Compound 3 has rigid molecules, obviously because of enhanced π-accepting properties and, therefore, greater equatorial preference of the N,C bound ketene imine ligands.

The reaction of equimolar amounts of the complex 1a or 1c with EtCN in ether at room temperature gave the thermally labile derivatives 4 and 5. The phosphite derivative 4 was found to be extremely sensitive and was characterized only by ^{1}H NMR spectroscopy. The structure of 5 was found to be 5a in the solid state by an X-ray structure analysis. However, we suggest that in solution, an equilibrium exists between two isomers with end-on and side-on bound nitrile ligands (eq. 1), of which 5b represents one of the rare cases of a mononuclear complex which contains an η^2-nitrile moiety [7]. The equilibrium between 5a and 5b can be detected by IR spectroscopy since two sets of ν(C≡O) and ν(C≡N) absorptions are present (see Table 1). Not much information about this isomerisation process can be extracted from the ^{1}H NMR spectrum because of overlapping resonances. In the spectrum of the dicarbonylpropionitrilebis(trimethylphosphite)iron complex 4, however, the res-

Table 1

IR [a] and ¹H NMR [b] data for complexes 2–5

	ν(CO), ν(CCO) or ν(CN)	δ	J (P–H,H–H) [c]	
2a,2d [d]	2024 s	7.9–7.05m		Ph
	2016 s	3.56t	5.5	$P(OCH_3)_3$
	1966 s			
	1959 s			
	1586 w,b			
2b,2e	2016 s	8.1–6.9m		Ph
	2009 s	4.6sept(t)	6.1(1.8)	PO–CH
	1955 s	1.24d	6.1	CH_3
	1945 s	1.11d	6.1	CH_3
	1586 w,b			
2c	1978 s	7.78d	7.3	
	1912 s	7.50d	7.3	
	1548 w,b	7.28t	7.3	Ph
		7.16t	7.3	
		7.05t	7.3	
		6.90t	7.3	
		1.63quint	2.7	P–CH_2–CH_3
		0.99sept	7.6	P–CH_2–CH_3
3	1990 s [e]	7.9–7.0m	10.9	Ph
	1934 s [e]	7.0–6.4m		C_6H_4
	2000 s	3.44t		OCH_3
	1935 s	2.11s		CH_3
4		3.70t	5.8	OCH_3
		1.25q(t)	7.7(<1)	P–CH_2–CH_3
		0.37t	7.1	P–CH_2–CH_3
5	1870 s [f]	1.72sept	4.1	P–CH_2–CH_3
	1902 s	1.22quint	7.3	P–CH_2–CH_3
	1816 s [f]	0.42t	7.6	CH_3
	1852 s			
	1625 s			
	2112 w [f]			

[a] cm⁻¹, n-pentane. [b] ppm from Me_4Si in CD_3COCD_3. [c] In Hz. [d] IR in ether. [e] In KBr. [f] Assigned to **5a**.

onance for the methylene protons is split by additional P-coupling. This could originate from contributions by **4b** in a fast rearrangement process on the NMR time scale. It could not easily be envisaged for species **4a**, since a five-bond coupling pathway would be required. The ³¹P NMR spectrum of **5** again gives evidence for two separate species, in an approximate ratio of 10/1 at −10°C.

The relevant ³¹P and ¹³C NMR data for complexes **2a**, **2b**, **2c**, **3**, **5a** and **5b** are given in Table 2.

Crystal and molecular structures of 2c, 3 and 5a [8*]

Crystals suitable for the X-ray analysis of **2c** (Fig. 1), and **5** (Fig. 3) were obtained by slowly cooling pentane solutions to −80°C, and crystals of **3** (Fig. 2)

---

* Reference number with asterisk indicates a note in the list of references.

Table 2

^{31}P and ^{13}C NMR data for the complexes 2–5

| | ^{31}P NMR ^{a} | ^{13}C NMR ^{b} | | |
		δ	J(P–C) ^{c}	Group
2a	152.0	198.2t	43.4	C≡O
		193.3t	29.3	C≡O
		157.5t	24.5	η^2-C=O
		143.1 141.4		Ph
		129.7 127.6		
		127.6 126.9		
		123.9 122.4		
		94.84		CPh$_2$
		39.6		OCH$_3$
2b	148.4	214.8t	42.3	C≡O
		209.9t	31.5	C≡O
		176.4t	22.6	η^2-C=O
		143.1 142.8		Ph
		128.9 127.4		
		127.0		
		122.9 121.8		
		92.2		CPh$_2$
		70.1		OCH
		23.9		CH$_3$
2c	44.5	218.6t	28.2	C≡O
		212.5t	21.1	C≡O
		179.5t	17.6	η^2-C=O
		143.4 141.8		Ph
		128.5 127.7		
		127.5 126.7		
		123.3 122.2		
		94.1		CPh$_2$
		16.7t	24.6	P–CH_2–CH$_3$
		7.5		P–CH$_2$–CH_3
3	157.4			
5a	68.7			
5b	50.7			

^{a} ppm from H$_3$PO$_4$ in CDCl$_3$, $-10\,^\circ$C. ^{b} ppm from Me$_4$Si in CDCl$_3$, $-10\,^\circ$C. ^{c} In Hz.

by the slow evaporation of a hexane solution at $5\,^\circ$C. The crystal parameters and the conditions of the measurements are listed in Table 3. The final refinement cycles led to the positional parameters of **2c**, **3** and **5a** given in Tables 4, 6 and 7, respectively.

Among ketene complexes whose structures have been determined by X-ray crystallography there are examples of η^2-C,C [3] and η^2-C,O [4] coordination. The spectroscopic data provide evidence that complexes **2** contain side-on C,O-bonded-ketene ligands and since this binding mode is not expected for non-oxophilic iron centres, we wanted to confirm the structure of **2c** by an X-ray analysis.

The coordination geometry around the iron centre of **2c** can be described as a trigonal bipyramid with the phosphane substituents in the axial and the η^2-C,O bound ketene system in the equatorial positions. The gross structural features of the metal ketene unit compare well with those of other related complexes [4a–4c] (see Table 5). The bending of the C$_2$O moiety at the internal C appears to be about

Table 3

Crystallographic and refinement data of **2c**, **3** and **5a** [9*]

	2c	**3**	**5a**
Formula	$C_{28}H_{40}FeO_3P_2$	$C_{29}H_{35}FeNO_8P_2$	$C_{17}H_{35}FeNO_2P_2$
Lattice constants by refinement of the diffractometer setting angles of 15 reflections with $11° < 2\theta < 23°$			
Cryst. system	triclinic	triclinic	monoclinic
Space group	$P\bar{1}$	$P\bar{1}$	$P2_1/c$
a, Å	9.714(4)	14.825(9)	12.236(4)
b, Å	10.065(4)	14.941(7)	7.921(3)
c, Å	14.768(7)	15.177(7)	20.176(8)
α, deg	90.55(4)	86.91(4)	
β, deg	98.10(4)	87.57(4)	106.56(3)
γ, deg	102.33(4)	73.56(4)	
Z	2	4	4
ρ (calcd), g cm^{-3}	1.29	1.33	1.43
Temp., °C	−39	20	−35
Crystal dimens., mm	$0.2 \times 0.3 \times 0.3$	$0.2 \times 0.1 \times 0.1$	$0.17 \times 0.28 \times 0.33$
Radiation	graphite monochromated Mo-K_α (λ 0.71073 Å)		
Abs. coeff., cm^{-1}	6.8	5.6	10.0
	three check intensities monitored periodically during data collection gave no indication for crystal decay.		
Scan speed, deg/min	2.0–29.3	4.0–29.3	2.2–29.3
2θ scan range, deg	$3 \leq 2\theta \leq 45$	$5 \leq 2\theta \leq 40$	$2 \leq 2\theta \leq 46$
Scan technique	ω-scan	$\theta/2\theta$	ω-scan
ω-scan range, deg	1.10		1.1
Total number of reflections measured	3890	6068	2530
Source of atomic scattering factors	atomic scattering factors from "International Tables" or from the sources given in the programs cited.		
Unique data with	3284	2235	1689
	$(F_o) \geq 2.5 \, \sigma(F_o)$	$(F_o) \geq 4 \, \sigma(F_o)$	$(F_o) \geq 4 \, \sigma(F_o)$
Data correction	data were corrected for Lorentz and polarization effects but not for absoprtion or extinction.		
Nature and refined parameters	all non-hydrogen atoms with anisotropic temperature factors	all non-hydrogen atoms with anisotropic temperature factors, phenyl rings as rigid groups	all non-hydrogen atoms with anisotropic temperature factors, PEt$_3$ carbon atoms with split occupancy factors of 0.5
Parameters refined	307	474	131
Structure solution		direct methods	
R_F	0.034	0.079	0.086
R_{F^2}	0.035	0.089	0.094

midway between the two extremes found for zirconium (123.6°) [4a] and vanadium ketene compounds (139.9°) [4b]. The length of the (C–O)(ketene) bond in **2c** is the shortest example in all of the structurally investigated η^2-C,O ketene complexes. This bond is even shorter than the corresponding one in the aldehyde compound $Fe(CO)_2[P(OMe)_3]_2CH_2O$ [1]. The iron–carbon separation in **2c** is significantly shorter than for the corresponding Fe–C bond in **3**. This may be caused, along with other influences, by the stronger polarization effect of the oxygen heteroatom in π-type wave functions. This leads to an increase of the carbon atom coefficients in

Table 4

Atomic coordinates with esd's for **2c**

	x	y	z
Fe(1)	0.2786(1)	0.1919(1)	0.2909(1)
C(1)	0.1140(4)	0.2082(3)	0.2348(2)
O(1)	0.0064(2)	0.2198(2)	0.1967(2)
C(2)	0.2361(3)	0.0289(3)	0.3388(2)
O(2)	0.2051(3)	−0.0757(2)	0.3678(2)
O(3)	0.4841(2)	0.2736(2)	0.3247(1)
C(3)	0.4220(3)	0.3467(3)	0.2697(2)
C(4)	0.4726(3)	0.4637(3)	0.2288(2)
C(5)	0.6243(3)	0.5270(3)	0.2459(2)
C(6)	0.6703(3)	0.6675(3)	0.2534(2)
C(7)	0.8119(4)	0.7283(3)	0.2686(2)
C(8)	0.9133(4)	0.6517(4)	0.2750(2)
C(9)	0.8700(4)	0.5132(4)	0.2673(3)
C(10)	0.7291(4)	0.4518(4)	0.2544(2)
C(11)	0.3785(3)	0.5214(3)	0.1601(2)
C(12)	0.4312(3)	0.5775(3)	0.0831(2)
C(13)	0.3425(4)	0.6206(3)	0.0135(2)
C(14)	0.2024(4)	0.6115(3)	0.0190(2)
C(15)	0.1492(3)	0.5601(3)	0.0957(2)
C(16)	0.2374(3)	0.5168(3)	0.1654(2)
P(1)	0.3225(1)	0.0994(1)	0.1630(1)
C(17)	0.2749(4)	0.1859(3)	0.0594(2)
C(18)	0.2978(4)	0.1250(4)	−0.0298(2)
C(19)	0.5073(4)	0.0976(3)	0.1620(2)
C(20)	0.5708(4)	0.0202(4)	0.2386(3)
C(21)	0.2337(4)	−0.0767(3)	0.1363(2)
C(22)	0.0744(4)	−0.0992(3)	0.1172(3)
P(2)	0.2469(1)	0.2912(1)	0.4204(1)
C(23)	0.1002(4)	0.2045(4)	0.4764(2)
C(24)	−0.0439(4)	0.1751(4)	0.4187(3)
C(25)	0.2224(3)	0.4646(3)	0.4108(2)
C(26)	0.2077(4)	0.5402(4)	0.4963(2)
C(27)	0.3990(4)	0.3085(4)	0.5092(2)
C(28)	0.4461(4)	0.1771(4)	0.5321(3)

π^{*} orbitals, with subsequent enhancement of their back-bonding interactions.

Since there are close structural and electronic similarities between the heteroallenic systems of ketenes and ketene imines, their coordination behaviour should also be closely related. In fact, the structure determination of **3** reveals an inner coordination geometry similar to that of **2c**. The unit cell of **3** contains two independent molecules, which show very similar structural features. The ketene imine ligand in **3** is bonded in an η^2-C,N fashion, although in some complexes η^1-nitrogen attachment has been observed [4a]. The bending that occurs at the internal C atom upon coordination is somewhat smaller than the corresponding angle in **2c** but is still in the range found in the structures of other ketene-imine complexes [4e,10]. As expected, in comparison to the C–N length in the free organic system (1.21 Å (molecule 1)) [11], a rather large elongation of the C–N bond (0.13 Å) accompanied the attachment of the ketene imine unit to the metal centre.

Table 5

Selected bond distances (Å) and angles (deg) with esd's for **2c**

Fe(1)–C(1)	1.735(3)	Fe(1)–C(2)	1.783(3)
Fe(1)–O(3)	1.980(2)	Fe(1)–C(3)	1.916(3)
Fe(1)–P(1)	2.231(1)	Fe(1)–P(2)	2.240(1)
C(1)–O(1)	1.145(4)	C(2)–O(2)	1.136(4)
O(3)–C(3)	1.276(3)	C(3)–C(4)	1.358(4)
C(4)–C(5)	1.460(4)	C(4)–C(11)	1.476(4)
C(5)–C(6)	1.388(4)	C(5)–C(10)	1.386(5)
C(6)–C(7)	1.367(4)	C(7)–C(8)	1.368(5)
C(8)–C(9)	1.366(5)	C(9)–C(10)	1.362(5)
C(11)–C(12)	1.388(4)	C(11)–C(16)	1.374(4)
C(12)–C(13)	1.380(4)	C(13)–C(14)	1.359(5)
C(14)–C(15)	1.371(5)	C(15)–C(16)	1.379(4)
P(1)–C(17)	1.820(3)	P(1)–C(19)	1.801(4)
P(1)–C(21)	1.810(3)	C(17)–C(18)	1.511(5)
C(19)–C(20)	1.514(6)	C(21)–C(22)	1.501(5)
P(2)–C(23)	1.814(4)	P(2)–C(25)	1.815(3)
P(2)–C(27)	1.810(3)	C(23)–C(24)	1.502(5)
C(25)–C(26)	1.508(5)	C(27)–C(28)	1.515(6)
C(1)–Fe(1)–C(2)	102.0(1)	C(1)–Fe(1)–O(3)	147.9(1)
C(2)–Fe(1)–O(3)	110.1(1)	C(1)–Fe(1)–C(3)	109.8(1)
C(2)–Fe(1)–C(3)	148.1(1)	O(3)–Fe(1)–C(3)	38.2(1)
C(1)–Fe(1)–P(1)	89.7(1)	C(2)–Fe(1)–P(1)	91.3(1)
O(3)–Fe(1)–P(1)	90.2(1)	C(3)–Fe(1)–P(1)	86.2(1)
C(1)–Fe(1)–P(2)	92.6(1)	C(2)–Fe(1)–P(2)	90.2(1)
O(3)–Fe(1)–P(2)	86.7(1)	C(3)–Fe(1)–P(2)	91.1(1)
P(1)–Fe(1)–P(2)	176.9(1)	Fe(1)–C(1)–O(1)	179.0(3)
Fe(1)–C(2)–O(2)	177.9(3)	Fe(1)–O(3)–C(3)	68.2(1)
Fe(1)–C(3)–O(3)	73.6(1)	Fe(1)–C(3)–C(4)	154.5(2)
O(3)–C(3)–C(4)	131.8(2)	C(3)–C(4)–C(5)	120.1(3)
C(3)–C(4)–C(11)	120.7(2)	C(5)–C(4)–C(11)	119.0(2)

The structure of complex **5** was determined because of the possibility of the η^2-coordination behavior of the nitrile molecule. It is interesting to note that isomere **5a** is the one preserved in the solid state (see Table 8). Complex **5a** was found to have a trigonal bipyramidal geometry, with the carbonyl and phosphane groupings occupying the same positions as in **2c**. The propionitrile ligand is attached to the iron centre in a linear fashion by η^1-nitrogen coordination and the bond distance lies in the same range as that determined for an L_4Fe acetonitrile system [12]. The major difference in coordination geometry when compared with **2c** lies in a wider Fe(CO)$_2$ angle. The C_{2v}-ML$_4$ fragments have two valence orbitals lying above the d block [13]. The lower-lying HOMO (low spin d^8 occupation) is asymmetric with respect to the plane containing the axial ligands. This orbital, which is involved in the back donation to π-acceptor ligands, can be raised in energy by bringing the equatorial L_2M angle closer to 90°. Such higher-lying functions should show enhanced interaction with accepting ligand orbitals located at elevated energy levels (e.g. the ketene ligand in **2**). In contrast, ligands with a low-lying accepting function as well as non-π-acceptor systems (e.g. an η^1-nitrile group as in **4**) cannot profit from higher energy π-donor orbitals and their bonding is, therefore, accompanied by relaxed equatorial Fe(CO)$_2$ angles.

Table 6

Atomic coordinates with esd's for **3**

Atom	Molecule 1			Atom	Molecule 2		
	x	y	z		z	y	z
Fe(11)	0.2146(3)	0.1354(3)	0.9370(2)	Fe(21)	−0.2885(3)	0.1312(2)	0.4241(2)
P(11)	0.1560(5)	0.2399(5)	0.8285(5)	P(21)	−0.2901(5)	0.0224(5)	0.5294(5)
P(12)	0.2757(6)	0.0277(5)	1.0416(5)	P(22)	−0.2843(5)	0.2384(4)	0.3177(4)
O(11)	0.128(1)	0.348(1)	0.8551(9)	O(21)	−0.344(2)	0.050(1)	0.622(1)
O(12)	0.072(1)	0.228(1)	0.774(1)	O(22)	−0.185(1)	−0.030(1)	0.566(1)
O(13)	0.231(1)	0.246(1)	0.7459(9)	O(23)	−0.321(1)	−0.060(1)	0.4946(9)
O(14)	0.313(3)	0.049(1)	1.125(2)	O(24)	−0.307(1)	0.342(1)	0.349(1)
O(15)	0.196(2)	−0.030(2)	1.087(2)	O(25)	−0.192(1)	0.225(1)	0.253(1)
O(16)	0.349(1)	−0.060(1)	1.002(1)	O(26)	−0.360(1)	0.252(1)	0.240(1)
O(17)	0.129(2)	−0.002(1)	0.863(1)	O(27)	−0.124(2)	−0.002(1)	0.347(2)
O(18)	0.404(1)	0.103(1)	0.856(1)	O(28)	−0.457(1)	0.104(1)	0.346(1)
N(11)	0.127(1)	0.198(1)	1.032(1)	N(21)	−0.238(1)	0.191(1)	0.523(1)
C(11)	0.201(2)	0.233(2)	1.023(1)	C(21)	−0.332(2)	0.229(2)	0.515(1)
C(12)	0.235(1)	0.296(2)	1.065(2)	C(22)	−0.404(2)	0.293(2)	0.558(1)
C(13)	0.3236(8)	0.3233(8)	1.0290(9)	C(23)	−0.5062(8)	0.3181(9)	0.525(1)
C(14)	0.3845(8)	0.3431(8)	1.0878(9)	C(24)	−0.5785(8)	0.3407(9)	0.589(1)
C(15)	0.4613(8)	0.3729(8)	1.0558(9)	C(25)	−0.6720(8)	0.3704(9)	0.563(1)
C(16)	0.4772(8)	0.3828(8)	0.9650(9)	C(26)	−0.6932(8)	0.3774(9)	0.474(1)
C(17)	0.4163(8)	0.3630(8)	0.9062(9)	C(27)	−0.6208(8)	0.3548(9)	0.410(1)
C(18)	0.3395(8)	0.3333(8)	0.9382(9)	C(28)	−0.5273(8)	0.3252(9)	0.436(1)
C(19)	0.1887(8)	0.337(1)	1.1508(7)	C(29)	−0.380(1)	0.329(1)	0.6393(8)
C(110)	0.1846(8)	0.428(1)	1.1702(7)	C(210)	−0.421(1)	0.423(1)	0.6556(8)
C(111)	0.1414(8)	0.465(1)	1.2488(7)	C(211)	−0.399(1)	0.460(1)	0.7318(8)
C(112)	0.1023(8)	0.411(1)	1.3081(7)	C(212)	−0.337(1)	0.403(1)	0.7917(8)
C(113)	0.1064(8)	0.319(1)	1.2886(7)	C(213)	−0.297(1)	0.309(1)	0.7755(8)
C(114)	0.1496(8)	0.282(1)	1.2100(7)	C(214)	−0.318(1)	0.272(1)	0.6993(8)
C(115)	0.0295(7)	0.249(1)	1.0308(8)	C(215)	−0.1668(8)	0.236(1)	0.5236(8)
C(116)	−0.0017(7)	0.346(1)	1.0348(8)	C(216)	−0.1839(8)	0.332(1)	0.5303(8)
C(117)	−0.0978(7)	0.392(1)	1.0357(8)	C(217)	−0.1089(8)	0.370(1)	0.5367(8)
C(118)	−0.1628(7)	0.340(1)	1.0325(8)	C(218)	−0.0167(8)	0.312(1)	0.5364(8)
C(119)	−0.1317(7)	0.243(1)	1.0285(8)	C(219)	0.0003(8)	0.216(1)	0.5297(8)
C(120)	−0.0355(7)	0.198(1)	1.0277(8)	C(220)	−0.0747(8)	0.178(1)	0.5233(8)
C(121)	−0.273(2)	0.389(2)	1.034(2)	C(221)	0.064(1)	0.355(2)	0.549(1)
C(122)	0.098(2)	0.429(2)	0.795(2)	C(222)	−0.449(2)	0.088(2)	0.626(2)
C(123)	−0.021(2)	0.237(2)	0.790(2)	C(223)	−0.147(2)	−0.021(2)	0.646(2)
C(124)	0.261(2)	0.163(2)	0.683(2)	C(224)	−0.319(2)	−0.144(2)	0.551(2)
C(125)	0.385(2)	0.089(2)	1.145(3)	C(225)	−0.309(2)	0.429(2)	0.292(2)
C(126)	0.123(3)	−0.019(3)	1.133(3)	C(226)	−0.100(2)	0.224(2)	0.282(2)
C(127)	0.397(2)	−0.143(2)	1.054(2)	C(227)	−0.352(2)	0.179(2)	0.176(2)
C(128)	0.165(2)	0.051(2)	0.891(2)	C(228)	−0.188(2)	0.052(2)	0.373(2)
C(129)	0.327(2)	0.115(2)	0.890(2)	C(229)	−0.389(2)	0.112(2)	0.379(2)

Experimental

General procedure and materials

All reactions were carried out under an atmosphere of dried and purified dinitrogen or argon. Solvents were dried by conventional methods, distilled and stored under argon. ^{1}H NMR spectra were obtained on a Bruker WM 250 FT

Table 7

Selected bond distances (Å) and angles (deg) with esd's for **3** (molecule 1)

Fe–P(1)	2.227(5)	P(1)–Fe–P(2)	178.5(2)
Fe–P(2)	2.224(6)	N–Fe–C(28)	107.0(7)
Fe–C(28)	1.80(2)	C(28)–Fe–C(29)	106.3(8)
Fe–C(29)	1.76(2)	C(29)–Fe–C(1)	107.5(8)
N–C(1)	1.34(2)	Fe–C(28)–O(7)	177(2)
N–C(15)	1.42(2)	Fe–C(29)–O(8)	177(2)
C(2)–C(9)	1.50(2)	N–C(1)–C(2)	138(2)
Fe–N	2.02(2)	C(1)–C(2)–C(3)	122(1)
Fe–C(1)	1.99(2)	C(3)–C(2)–C(9)	120(2)
C(28)–O(7)	1.15(3)	N–Fe–C(1)	39.2(6)
C(29)–O(8)	1.18(2)	Fe–N–C(1)	69.2(8)
C(1)–C(2)	1.38(2)	Fe–C(1)–N	71.6(8)
C(2)–C(3)	1.55(2)	C(1)–N–C(15)	128(1)
C(18)–C(21)	1.56(2)	C(1)–C(2)–C(9)	119(1)
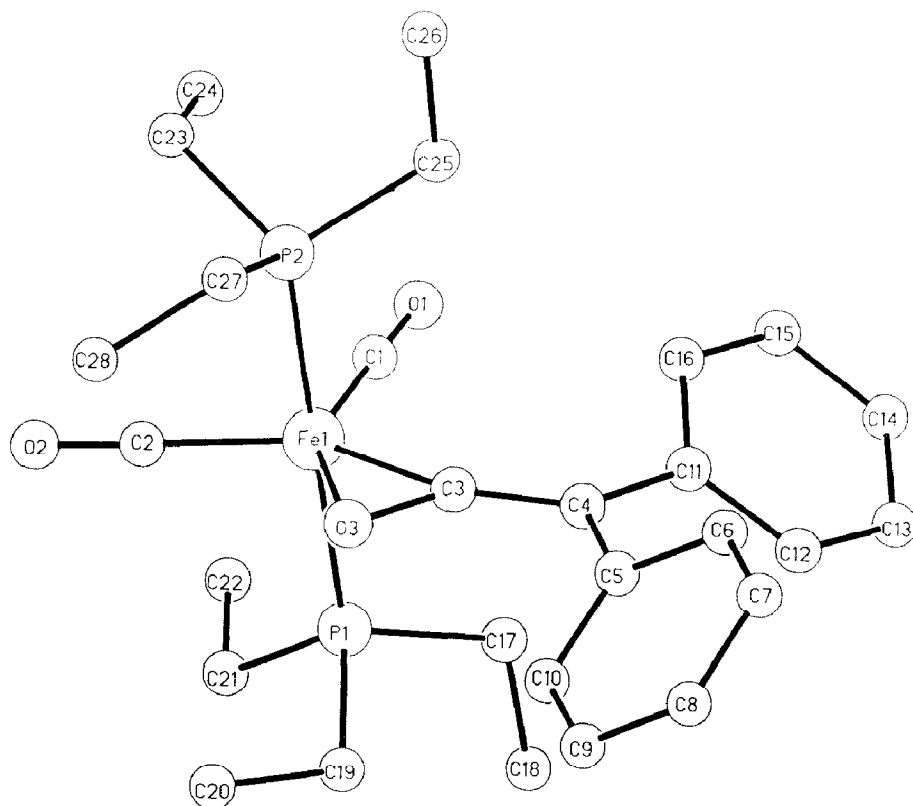
Fig. 1. Molecular structure of $Fe(CO)_2[PEt_3]_2Ph_2C_2O$ (**2c**).
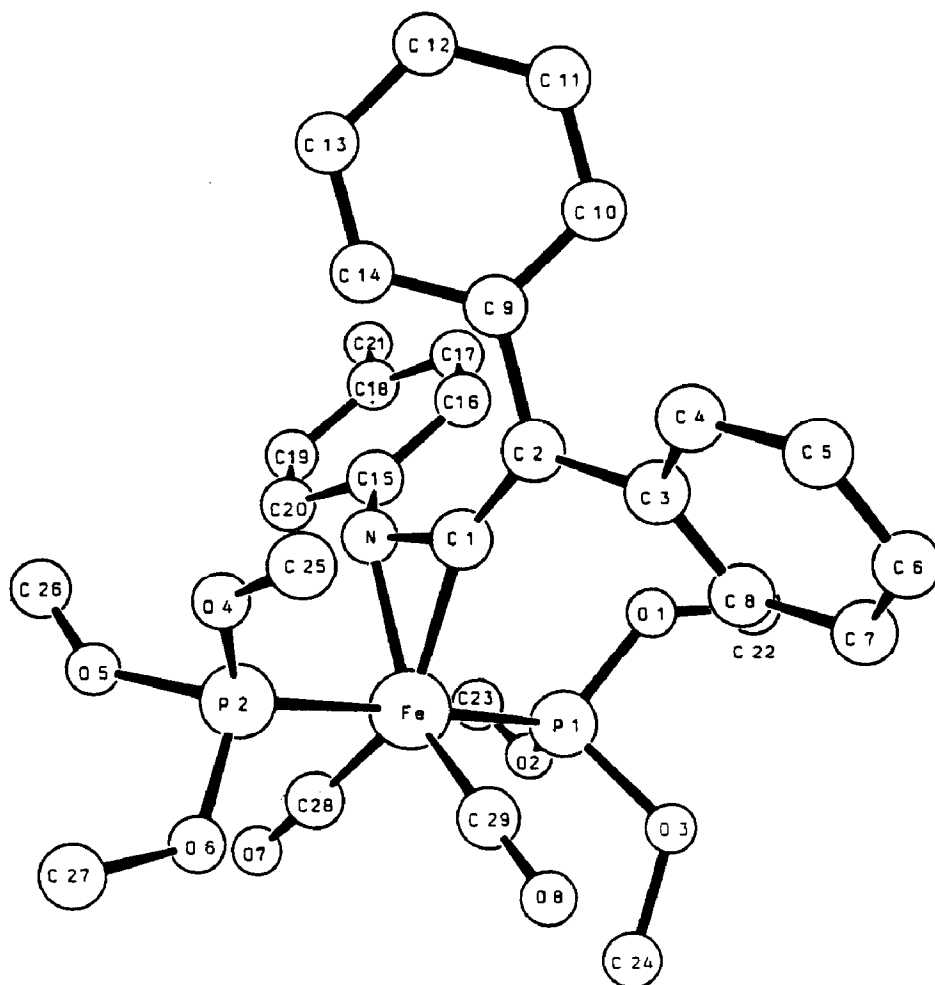
Fig. 2. Molecular structure of Fe(CO)$_2$[P(OMe)$_3$]$_2$Ph$_2$C$_2$N-p-tolyl (3) (molecule 1).

spectrometer using deuterated solvents as internal standards (δ acetone-d_6 2.04 ppm, C$_6$D$_6$ 7.15 ppm). Infrared spectra were obtained on a Zeiss IMR 40 spectrometer. Mass spectra were obtained using Finnigan MAT 112 or MAT 312 spectrometers at 70 eV.

The starting materials, (OC)$_3$FeL$_2$ (L = P/(OMe)$_3$, L = PEt$_3$), were synthesized by the reduction of (OC)$_2$FeL$_2$I$_2$ compounds with an excess of sodium sand in diethyl ether under 1 atm of CO. NaI and excess sodium were filtered off and the solvent was removed under vacuum, and (OC)$_3$Fe[P(OMe)$_3$]$_2$ and (CO)$_3$Fe(PEt$_3$)$_2$ were crystallised from ether and from pentane, respectively, at $-80\,^\circ$C. Diphenyl-ketene was obtained by a procedure cited in the literature [14].

[(OC)$_2$L$_2$Fe]$_2$N$_2$ (L = P(OMe)$_3$, 1a; L = PEt$_3$, 1c)

Fe(CO)$_3$L$_2$ (5 g) was irradiated for 2 h in 300 ml of diethyl ether (L = P(OMe)$_3$) or pentane (L = PEt$_3$) at $-20\,^\circ$C under a steady flow of nitrogen. The irradiation was continued at $-70\,^\circ$C for a further 12 h. The μ-dinitrogen complexes precipitated out as yellow microcrystalline solids. The solvent was decanted off to give the
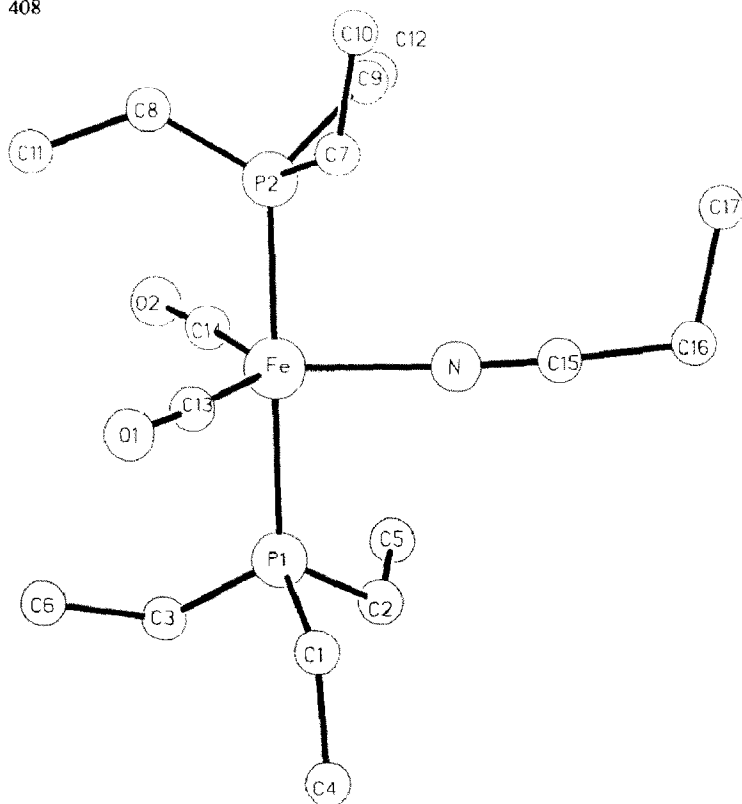
Fig. 3. Molecular structure of $Fe(CO)_2[PEt_3]_2 EtCN$ (**5a**).

Table 8

Atomic coordinates for **5a**

	x	y	z
Fe(1)	0.2435	0.1616	0.1096
P(1)	0.3008	0.2379	0.0234
P(2)	0.1883	0.0828	0.1959
O(1)	0.3508	−0.1635	0.1117
O(2)	0.0105	0.2139	0.0289
N(1)	0.3295	0.3457	0.1647
C(1)	0.4288	0.2051	0.0324
C(2)	0.2993	0.4348	0.0045
C(3)	0.2364	0.1753	−0.0509
C(4)	0.4892	0.2428	−0.0171
C(5)	0.2036	0.5294	−0.0039
C(6)	0.2060	0.0047	−0.0643
C(7)	0.2861	0.0478	0.2631
C(8)	0.1064	−0.0641	0.1917
C(9)	0.1390	0.2314	0.2373
C(10)	0.2685	0.0107	0.3285
C(11)	0.0858	−0.1971	0.1466
C(12)	0.0536	0.3463	0.2032
C(13)	0.3111	−0.0287	0.1120
C(14)	0.1026	0.2008	0.0614
C(15)	0.3767	0.4514	0.1985
C(16)	0.4372	0.5801	0.2466
C(17)	0.3893	0.5844	0.3084

samples of **1a** and **1c** used in the further reactions. Somewhat purer products were obtained, in yield of ca. 60%, by recrystallising **1a** (from ether) and **1c** (from pentane) at $-80°C$.

{(OC)₂[P(O-i-Pr)₃]₂Fe}₂N₂ (1b)

{(OC)$_2$[P(O-i-Pr)$_3$]$_2$Fe}$_2$N$_2$ (1b)

$Fe(CO)_2[P(O-i-Pr)_3]_2I_2$ (2 g) was reduced under nitrogen with activated magnesium in diethyl ether at $-20°C$ for approx. 12 h. Filtration through silica gel at $-20°C$ gave solution of **1b**, which was used in further reactions.

(OC)₂L₂FePh₂C₂O (L = P(OMe)₃, 2a: L = P(O-i-Pr)₃, 2b; L = PEt₃, 22)

(OC)$_2$L$_2$FePh$_2$C$_2$O (L = P(OMe)$_3$, 2a: L = P(O-i-Pr)$_3$, 2b; L = PEt$_3$, 22)

1 (3 mmol) was dissolved at $-20°C$ in 100 ml diethyl ether and 1.15 g (6 mmol) diphenylketene was added. The reaction was stirred at room temperature for 4 h, the solvent was removed, and the residue was extracted with pentane (**2a,2b**) or diethyl ether (**2c**). The compounds **2** were obtained as red crystals in quantitative yields.

2a: Found: C, 47.65; H, 5.05. $C_{22}H_{28}FeO_9P_2$ calcd.: C, 47.62; H, 4.86%. MS (130°C): $m/e = 554$ $[M]^+$, 388 $[M - Ph_2C]^+$, 360 $[M - Ph_2C_2O]^+$, 332 $[M - Ph_2C_2O, - CO]^+$, 304 $[FeL_2]^+$, 289 $[FeL_2 - Me]^+$, 273 $[FeL_2 - OMe]^+$, 258 $[FeL_2 - OMe, - Me]^+$, 242 $[FeL_2 - 2OMe]^+$, 227 $[FeL_2 - 2OMe, - Me]^+$, 211 $[FeL_2 - 3OMe]^+$, 180 $[FeL]^+$.

2b: Anal. Found: C, 56.53; H, 7.20. $C_{34}H_{52}FeO_9P_2$ calcd.: C, 56.52; H, 7.25%. MS (110°C): $m/e = 542$ $[M]^+$, 376 $[M - Ph_2C]^+$, 348 $[M - Ph_2C_2O]^+$, 320 $[M - Ph_2C_2O, - CO]^+$, 292 $[FeL_2]^+$, 174 $[FeL]^+$.

2c: Found: C, 62.32; H, 7.69. $C_{28}H_{40}FeO_3P_2$ calcd.: C, 62.00; H, 7.43%. MS (80°C): $m/e = 722$ $[M]^+$, 528 $[M - Ph_2C_2O]^+$, 500 $[M - Ph_2C_2O, - CO]^+$, 472 $[FeL_2]^+$, 429 $[FeL_2 - C_3H_7]^+$, 371 $[FeL_2 - O-i-Pr, - C_3H_6]^+$, 323 $[FeLP]^+$.

(OC)₂[P(OMe)₃]₂FePh₂C₂N-p-tolyl (3)

(OC)$_2$[P(OMe)$_3$]$_2$FePh$_2$C$_2$N-p-tolyl (3)

1a (3.6 mmol) in 150 ml ether was chilled to $-30°C$ and 0.23 g (0.81 mmol) of Ph_2C_2N-p-tolyl in 10 ml ether was added. Slow warming to room temperature caused the colour to change from light yellow to orange. The mixture was stirred for 20 h, the solvent was removed by evaporation and the oily residue extracted with ether (30°C). The solution was filtered and cooled to $-40°C$ for 3 d to give crystals of **3**. Yield 0.28 g (60%). M.p. 114°C. Anal. Found: C, 54.30; H, 5.59; N, 2.20. $C_{29}H_{35}FeNO_8P_2$ calcd.: C, 54.13; H, 5.48; N, 2.18%.

(OC)₂L₂FeNCEt (L = P(OMe)₃, 4a; L = PEt₃, 5a)

(OC)$_2$L$_2$FeNCEt (L = P(OMe)$_3$, 4a; L = PEt$_3$, 5a)

1a or **1c** (2 g, 2.8 mmol) and a threefold excess of freshly distilled propionitrile in 100 ml diethyl ether were mixed at $-20°C$ and then stirred for 4 h at room temperature. The solvent was removed and the oily residues extracted with ether (**4**) or pentane (**5**). Crystallisation at $-80°C$ gave yellow crystals of **4** (yield 60%) or **5** (yield 62%).

410

References

1 H. Berke, W. Bankhardt, G. Huttner, J. v. Seyerl L. Zsolnai, Chem. Ber., 114 (1981) 2754.

2 H. Berke, R. Birk, G. Huttner, L. Zsolnai, Z. Naturforsch. B, 39 (1984) 1380.

3 K. Schorpp, W. Beck, Z. Naturforsch. B, 28 (1973) 738; W.A. Herrmann, Angew. Chem., Int. Ed. Engl., 13 (1974) 335; A.D. Redhouse, W.A. Herrmann, ibid., 15 (1976) 615; W.A. Herrmann, J. Plank, ibid., 17 (1978) 525; W.A. Herrmann, J. Plank, M.L. Ziegler, K. Weidenhammer, J. Am. Chem. Soc., 101 (1979) 3133; A. Miyashita, R.H. Grubbs, Tetrahedron Lett., 22 (1981) 1255.

4 (a) G.S. Bristow, P.B. Hitchcock, M.F. Lappert, J. Chem. Soc., Chem. Commun., (1982) 462; (b) S. Gambarotta, M. Pasquali, C. Floriani, C. Guastini, A. Chiesi-Villa, Inorg. Chem., 20 (1981) 1173 and lit. cit.; (c) G. Fachinetti, C. Biran, C. Floriani; A. Chiesi-Villa, C. Guastini, ibid., 17 (1978) 2995; (d) D.A. Straus, R.H. Grubbs, J. Am. Chem. Soc., 104 (1982) 5499; (e) Th. Sielisch, U. Behrens, J. Organomet. Chem., 310 (1986) 179.

5 R. Birk, H. Berke, G. Huttner, L. Zsolnai, J. Organomet. Chem., 309 (1986) C18.

6 (a) B. Bogdanovic, S. Liao, M. Schwickardi, P. Sikorsky, B. Spliethoff, Angew. Chem., Int. Ed. Engl., 19 (1980) 818; (b) P. Conway, S.M. Grant, A.R. Manning, F.S. Stephens, Inorg. Chem., 22 (1983) 3714.

7 B.N. Storhoff, C.L. Huntley, Jr., Coord. Chem. Rev., 23 (1977) 1; T.C. Wright, G. Wilkinson, M. Motevalli, M.B. Hursthouse, J. Chem. Soc., Dalton Trans., (1986) 2017; J.L. Thomas, J. Am. Chem. Soc., 97 (1975) 5943; W.J. Bland, R.D.W. Kemmitt, R.D. Moore, J. Chem. Soc. Dalton Trans., (1973) 1292.

8 Additional information may be obtained from Fachinformationszentrum Energie Physik Mathematik, D-7514 Eggenstein-Leopoldshafen 2, FRG. Orders should refer to deposit number CSD 53711 and this manuscript.

9 (a) Programs used for 2c: G.M. Sheldrick, Crystallographic Computing System SHELXTL, Revision 1982, University of Göttingen, F.R.G.; (b) for 3: G.M. Sheldrick, SHELX-76, Programs for Crystal Structure Determination, University of Cambridge (U.K.), 1976; (c) for 5a: S.R. Hall, J.M. Stewart, XTAL 83 System of Crystallographic Programs, 1983, University of Western Australia, Wedlands, Australia 6009.

10 D.J. Yarrow, J.A. Ibers, Y. Tatsuno, S. Otsuka, J. Am. Chem. Soc., 95 (1973) 8590.

11 R.R. Naqvi, P.J. Wheatley, J. Chem. Soc. A, (1970) 2053.

12 V.L. Goedken, Y. Park, S.-M. Peng, J.A. Molin Norris, J. Am. Chem. Soc., 96 (1974) 7693.

13 M. Elian, R. Hoffmann, Inorg. Chem., 14 (1975) 1058.

14 E.C. Taylor, A. McKillop, G.H. Hawks, Org. Syntheses, 1972, 36; C.L. Stevens, G.H. Singhal, J. Org. Chem., 29 (1964) 34; H.J. Bestmann, J. Lienert, L. Mott, Liebigs Ann. Chem., 718 (1968) 24.